

INFNFE-02-98
BARI-TH/297-98
OUTP-98-14-P
astro-ph/9803177

Quantifying uncertainties in primordial nucleosynthesis without Monte Carlo simulations

G. Fiorentini ^a, E. Lisi ^b, S. Sarkar ^c, and F. L. Villante ^a

^a*Dipartimento di Fisica and Sezione INFN di Ferrara, Via del Paradiso 12, I-44100 Ferrara, Italy*

^b*Dipartimento di Fisica and Sezione INFN di Bari, Via Amendola 173, I-70126 Bari, Italy*

^c*Theoretical Physics, University of Oxford, 1 Keble Road, Oxford OX1 3NP, UK*

Abstract

We present a simple method for determining the (correlated) uncertainties of the light element abundances expected from big bang nucleosynthesis, which avoids the need for lengthy Monte Carlo simulations. Our approach helps to clarify the role of the different nuclear reactions contributing to a particular elemental abundance and makes it easy to implement energy-independent changes in the measured reaction rates. As an application, we demonstrate how this method simplifies the statistical estimation of the nucleon-to-photon ratio through comparison of the standard BBN predictions with the observationally inferred abundances.

26.35.+c, 98.80.Ft

Typeset using REVTEX

I. INTRODUCTION

Big bang nucleosynthesis is entering the precision era [1]. On the one hand, there has been major progress in the observational determination of the abundances of the light elements D [2,3], ^3He [4,5], ^4He [6,7], and ^7Li [8,9], although the increasing precision has highlighted discrepancies between different measurements (see Refs. [10–12] for recent assessments). Secondly, we have a sound analytical understanding of the physical processes involved [13,14] and the standard BBN computer code [15,16] which incorporates this physics is robust and can be easily altered to accomodate changes in the input parameters, e.g. nuclear reaction rates [17]. The comparison of increasingly accurate observationally inferred and theoretical abundances will further constrain the values of fundamental parameters, such as the nucleon density parameter (see, e.g., Ref. [18]) or extra degrees of freedom related to possible new physics beyond the Standard Model (see, e.g., Ref. [19]). It goes without saying that error evaluation represents an essential part of such comparisons.

Because of the complex interplay between different nuclear reactions, it is not straightforward to assess the effect on a particular elemental yield of the uncertainties in the experimentally determined reaction rates. The authors of Ref. [20] first employed Monte Carlo methods to sample the error distributions of the relevant reaction cross-sections which were then used as inputs to the standard BBN computer code. This enables well-defined confidence levels to be attached to the theoretically predicted abundances, e.g. the abundance range within which say 95% of the computed values fall correspond to 95% C.L. limits on the expected abundance. It was later realized that error correlations are also relevant, and can be estimated with the same technique [21,22]. The Monte Carlo (MC) approach has since become the standard tool for comparing theory and data [17,23–26]. However, although it can include refinements such as asymmetric or temperature-dependent reaction rate uncertainties [17], it requires lengthy calculations which need to be repeated each time (any of) the input parameters are changed or updated. Since we may expect further improvement in the determination of the relevant parameters, it is desirable to have a faster method for error evaluation and comparison with observations.

In this work we propose a simple method for estimation of the BBN abundance uncertainties and their correlations which requires little computational effort. The method, based on linear error propagation, is described in Sec. II. A concrete application is given in Sec. III, where theory and observations are compared using simple χ^2 statistics to obtain the best-fit value of the nucleon-to-photon ratio. In Sec. IV we study with this method the relative importance of different nuclear reactions in determining the synthesized abundances. Conclusions and perspectives for further work are presented in Sec. V.

II. PROPAGATING INPUT CROSS SECTION UNCERTAINTIES TO OUTPUT ELEMENTAL ABUNDANCES

A. Notation and input

The four relevant element abundances Y_i considered in this work are defined in Table I. (Note that the abundance of ^4He is conventionally quoted as a *mass fraction*, while the

abundances of D, ^3He and ^7Li are ratios by number.) In BBN calculations, the Y_i 's depend both on model parameters (the nucleon-to-photon ratio η , the number of neutrino families N_ν , etc.) and on a network of nuclear reactions R_k :

$$Y_i = Y_i(\eta, N_\nu, \dots; \{R_k\}) . \quad (1)$$

The most important R_k 's are listed, numbered as in Ref. [16], in the first two columns of Table II, while our default inputs for the rates R_k and their 1σ uncertainties $\pm\Delta R_k$ are given in the third and fourth columns. The numerical values are given in ratio to the reference reaction rates compiled in Table 1 of Ref. [17]; we have chosen identical values (i.e., $R_k = 1$) except for R_1 , the neutron decay rate, where we adopt the most recent world average for the neutron lifetime of $\tau_n = 886.7 \pm 1.9$ s [27,28], as compared to the value of $\tau_n = 888.54 \pm 3.73$ s used in Ref. [17]. The fractional uncertainties $\pm\Delta R_k/R_k$ ($k \neq 1$) have also been taken from Ref. [17] (see their Table 2), assuming conservatively the largest value for the temperature-dependent errors ΔR_7 and ΔR_{10} .¹

B. The method

For simplicity we consider only the standard BBN case (i.e., $N_\nu = 3$, etc.), so that η is the only model parameter being varied in the calculation of the abundances Y_i and of their uncertainties σ_i :

$$Y_i = Y_i(\eta) \pm \sigma_i(\eta) . \quad (2)$$

Our method can however be easily generalized to nonstandard cases.

For a relatively small change δR_k of the input rate R_k ($R_k \rightarrow R_k + \delta R_k$), the corresponding deviation δY_i of the i -th elemental abundance ($Y_i \rightarrow Y_i + \delta Y_i$), as given by linear propagation, reads

$$\delta Y_i(\eta) = Y_i(\eta) \sum_k \lambda_{ik}(\eta) \frac{\delta R_k}{R_k} , \quad (3)$$

where the functions $\lambda_{ik}(\eta)$ represent the logarithmic derivatives of Y_i with respect to R_k :

$$\lambda_{ik}(\eta) = \frac{\partial \ln Y_i(\eta)}{\partial \ln R_k(\eta)} . \quad (4)$$

In general, the deviations δY_i in Eq. (3) are correlated, since they all originate from the same set of reaction rate shifts $\{\delta R_k\}$. The global information is contained in the error matrix (also called covariance matrix) [29], which is a generalization of the “error vector” δY_i in Eq. (3). In particular, the abundance error matrix $\sigma_{ij}^2(\eta)$ obtained by linearly propagating the input $\pm 1\sigma$ reaction rate uncertainties $\pm\Delta R_k$ to the output abundances Y_i reads:

¹Our method for error propagation requires that the ΔR_k 's be constant (i.e., temperature independent). We will comment on this point at the end of this Section.

$$\sigma_{ij}^2(\eta) = Y_i(\eta)Y_j(\eta) \sum_k \lambda_{ik}(\eta)\lambda_{jk}(\eta) \left(\frac{\Delta R_k}{R_k}\right)^2. \quad (5)$$

This matrix completely defines the abundance uncertainties. In particular, the 1σ abundance errors σ_i of Eq. (2) are given by the square roots of the diagonal elements,

$$\sigma_i(\eta) = \sqrt{\sigma_{ii}^2(\eta)}, \quad (6)$$

while the error correlations ρ_{ij} can be derived from Eqs. (5,6) through the standard definition

$$\rho_{ij}(\eta) = \frac{\sigma_{ij}^2(\eta)}{\sigma_i(\eta)\sigma_j(\eta)}. \quad (7)$$

Thus Eqs.(2–7) represent all that is required to calculate the errors in the predicted abundances and their correlations.

Note that the relevant physics is contained entirely in the central values Y_i and in their logarithmic derivatives λ_{ik} , which have to be evaluated just once with a BBN numerical code, thus dramatically reducing the required computing time.² We have made a further check of the linearity of the error propagation by calculating the logarithmic derivatives with increments equal to ΔR_k (default) and $2\Delta R_k$, obtaining practically the same functions λ_{ik} in either case. This means that doubling the error on R_k also doubles the corresponding error component of Y_i , i.e. the error propagation is indeed linear.

We think it useful to present the results of this exercise in the form of tables so all calculations that will now follow can be done on a pocket calculator. Tables III and IV show the coefficients of polynomial fits to Y_i and λ_{ik} , respectively, for η in the usually considered range $10^{-10} – 10^{-9}$.³ The abundances $Y_i(\eta)$ with their associated ± 2 standard deviation error bands calculated through Eq. (6) are shown in Fig. 1. The functions $\lambda_{ik}(\eta)$ are shown in Fig. 2; note that some of these vary strongly (and even change sign) with η , indicating that the physical dependence of the Y_i ’s on the R_k ’s may be quite subtle. Although some general features of this dependence have been addressed in Ref. [14], further work is needed to interpret the functional form of the λ_{ik} ’s in Fig. 2. We intend to address this issue elsewhere. Finally, Fig. 3 displays the fractional uncertainties σ_i/Y_i and their correlations ρ_{ij} as derived from Eqs. (5–7). Notice that, in general, the error correlations are non-negligible and should be properly taken into account in statistical analyses, as first emphasized in Ref. [21].

²The logarithmic derivatives are numerically defined as $\lambda_{ik}(\eta) = [Y_i(\eta, R_k + \Delta R_k) - Y_i(\eta, R_k - \Delta R_k)]R_k/2Y_i(\eta, R_k)\Delta R_k$, at given η . We find negligible difference between left and right derivatives.

³Small corrections to the helium abundance Y_4 due to Coulomb, radiative and finite temperature effects, finite nucleon mass effects and differential neutrino heating, have been incorporated according to the prescription given in Ref. [19]. We have used the BBN code [16] with the lowest possible settings of the time steps in the (2nd order) Runge-Kutta routine, which allows rapid convergence to within 0.01% of the true value [30]. We understand that our results are in good agreement with a recent independent computation of Y_4 using a new BBN computer code [31].

In summary, the recipe for evaluating the BBN uncertainties $\pm\sigma_i$ affecting the Y_i 's for a given value of η is:

- (i) Determine the abundances $Y_i(\eta)$ and their logarithmic derivatives $\lambda_{ik}(\eta)$ using Tables III and IV, respectively;
- (ii) If the central values of the reaction rates R_k are updated ($R_k \rightarrow R_k + \delta R_k$) with respect to those reported in Table II, then update also the central values of the abundances ($Y_i \rightarrow Y_i + \delta Y_i$) through Eq. (3);
- (iii) For given reaction rate uncertainties ΔR_k (e.g., from Table III), compute the abundance errors σ_i and their correlations ρ_{ij} using Eqs. (5–7).

C. Comparison with MC estimates and remarks

Our approach is based on the linear propagation of errors originating from many independent sources (i.e. the R_k 's). One can expect that this method will work reasonably well, both because the input fractional uncertainties $\Delta R_k/R_k$ are relatively small, and because the final output uncertainties σ_i affecting the abundances Y_i are “regularized” by the central limit theorem. Indeed, our $\pm 2\sigma$ bands in Fig. 1 compare well with the MC-estimated bands of Refs. [17,21,23–26], with small relative differences which depend, in part on different input $R_k \pm \Delta R_k$'s, and that are not larger than the spread among the various MC estimates themselves.

In order to be more quantitative, we compare in Fig. 4 (upper panel) the MC evaluation of the fractional uncertainties σ_i/Y_i as derived from Ref. [17]⁴ with our analytic estimate (using, for this exercise, the same input parameters). There is good agreement between these two totally independent estimates. In Fig. 4 (lower panel) we also show a comparison with the only MC evaluation of ρ_{ij} we are aware of (viz., Ref. [22]), obtaining again good agreement with our calculation when the same input $R_k \pm \Delta R_k$ are used. We conclude the discussion of Fig. 4 by noting that the uncertainty $\sigma_{(2+3)}$ and the correlations $\rho_{(2+3)j}$ related to the often-used combination of abundances $Y_{(2+3)} = Y_2 + Y_3 = (\text{D} + {}^3\text{He})/\text{H}$ are given, within our approach, by:

$$\sigma_{(2+3)}^2 = \sigma_2^2 + \sigma_3^2 + 2\rho_{23}\sigma_2\sigma_3 , \quad (8)$$

$$\rho_{(2+3)j}\sigma_{(2+3)}\sigma_j = \rho_{2j}\sigma_2\sigma_j + \rho_{3j}\sigma_3\sigma_j . \quad (9)$$

There are, of course, some refined features of the MC approach that cannot be addressed with our method, such as asymmetric or temperature-dependent uncertainties ΔR_k [17]. However we consider these refinements not essential for practical applications. In a sense, the possible asymmetry between “upper” and “lower” errors is where one wants it to be. For

⁴The MC values of σ_i/Y_i have been read off the (small) panels of Fig. 27 in Ref. [17] and, therefore, may be subject to small transcription errors.

instance, if one assumes *a priori* symmetric errors in the astrophysical S -factors, then asymmetric errors are induced in the thermally averaged reaction rates $R \sim \langle \sigma v \rangle$; conversely, the requirement of *a priori* symmetric ΔR_k errors requires that the input S -factor uncertainties are readjusted, as discussed in Ref. [17]. Although the authors of Ref. [17] have adopted the latter option ($| + \Delta R_k | = | - \Delta R_k |$), the former option or others are equally acceptable, and would clearly produce different outputs for the MC estimate of the abundance errors. For instance, the upper and lower errors of Y_7 appear to be rather symmetrical in the MC calculation of Ref. [17], while they are noticeably asymmetrical in Ref. [22].

Concerning the temperature-dependent [17] uncertainties ΔR_7 and ΔR_{10} , which affect mainly the estimate of Y_7 , our conservative choice in Table II proves to be successful for the estimate of σ_7/Y_7 (see Fig. 4). This seems to indicate that the uncertainties at low temperatures (which are larger than those at high temperatures [17]) dominate in the estimate of these errors. In any case, since practically all reaction rate uncertainties ΔR_k contribute to the final value of σ_7 , temperature-dependent refinements in the propagation of just two of these (ΔR_7 and ΔR_{10}) do not appear to be decisive for the estimate of the global error σ_7 .

In conclusion, we have shown that our simple analytic method for error evaluation represents an useful alternative to lengthy and computationally expensive MC simulations. Both the magnitude and the correlations of the total errors affecting the theoretical abundances are reproduced with good accuracy. We therefore advocate the use of this method for BBN analyses as an alternative to MC simulations.⁵

III. DETERMINING THE LIKELY NUCLEON-TO-PHOTON RATIO

The comparison of the predicted primordial abundances $Y_i(\eta) \pm \sigma_i(\eta)$ with their observationally inferred values $\bar{Y}_i \pm \bar{\sigma}_i$ through a statistical test allows extraction of the likelihood range for the fundamental parameter η . So far, this has been done either through fit-by-eye (see, e.g., Ref. [17]) or by Monte Carlo-based maximum likelihood methods (see, e.g., Refs. [25,26]). In this Section we show how limits on η can be simply extracted using χ^2 statistics based on the method described in the previous Section.

Assuming that the errors $\bar{\sigma}_i$ in the determinations of different abundances \bar{Y}_i are uncorrelated, the experimental squared error matrix $\bar{\sigma}_{ij}^2$ is simply

$$\bar{\sigma}_{ij}^2 = \delta_{ij} \bar{\sigma}_i \bar{\sigma}_j , \quad (10)$$

where δ_{ij} is Kronecker's delta. The total (experimental + theoretical) error matrix S_{ij}^2 is then obtained by summing the matrices in Eqs. (5,10):

$$S_{ij}^2(\eta) = \sigma_{ij}^2(\eta) + \bar{\sigma}_{ij}^2 . \quad (11)$$

⁵ A parallel situation holds in the field of solar neutrino physics, where the correlated uncertainties of the neutrino fluxes predicted by solar models have been estimated through both Monte Carlo simulations [32] and linear propagation of input errors [33]. The latter technique has proved more popular because of its ease of use.

Its inverse defines the weight matrix $W_{ij}(\eta)$:

$$W_{ij}(\eta) = [S_{ij}^2(\eta)]^{-1}. \quad (12)$$

The χ^2 statistic associated with the difference between theoretical (Y_i) and observational (\bar{Y}_i) light element abundance determinations is then [29]:

$$\chi^2(\eta) = \sum_{ij} [Y_i(\eta) - \bar{Y}_i] \cdot W_{ij}(\eta) \cdot [Y_j(\eta) - \bar{Y}_j]. \quad (13)$$

Minimization of the χ^2 gives the most probable value of η , while the intervals defined by $\chi^2 = \chi_{\min}^2 + \Delta\chi^2$ give the likely ranges of η at the confidence level set by $\Delta\chi^2$ (for one degree of freedom, η).⁶

In order to illustrate this, we estimate η using recent observational data for the three light element abundances (Y_2, Y_4, Y_7) whose primordial origin is most secure. It is well known that the observationally inferred values \bar{Y}_2 and \bar{Y}_4 are still controversial, and the conflict between different determinations has driven a lively debate on the status of BBN (see Refs. [18,34] and references therein). In this paper we do not enter into this debate but rather apply our method to two possible (although mutually incompatible) selections of measurements which we name data set “A” and data set “B”:

$$\text{Data set A : } \begin{cases} \bar{Y}_2 = 1.9 \pm 0.4 \times 10^{-4}, \\ \bar{Y}_4 = 0.234 \pm 0.0054, \\ \bar{Y}_7 = 1.6 \pm 0.36 \times 10^{-10}; \end{cases} \quad (14)$$

$$\text{Data set B : } \begin{cases} \bar{Y}_2 = 3.40 \pm 0.25 \times 10^{-5}, \\ \bar{Y}_4 = 0.243 \pm 0.003, \\ \bar{Y}_7 = 1.73 \pm 0.12 \times 10^{-10}. \end{cases} \quad (15)$$

The data set “A” is used in Ref. [26], the authors of which make a detailed MC-based fit to η , thus enabling comparison with our method. Note that their adopted value of the primordial deuterium abundance from observations of high redshift quasar absorption systems is consistent with another recent observation, $\bar{Y}_2 = (2.15 \pm 0.35) \times 10^{-4}$ [3], but in conflict with the significantly smaller value reported in Ref. [2], which we adopt for data set “B”. Similarly the primordial helium mass fraction inferred from observations of metal-poor blue compact galaxies which we adopt for data set “B” is from Ref. [7] in which it is argued that previous analyses leading to the smaller value of \bar{Y}_2 used in data set “A” underestimate the true abundance (although this is disputed in Ref. [6].) Finally the estimates for the primordial lithium abundance in both data sets are based on observations of pop II stars, with the slightly higher value [9] of \bar{Y}_7 in data set “B” taken from an updated analysis. Readers who prefer to adopt different combinations of these, or indeed other, estimates for

⁶We remind the reader that $\Delta\chi^2 = 1, 2.71, 3.84$, and 6.64 correspond to confidence levels (C.L.’s) of 68%, 90%, 95%, and 99%, respectively.

the primordial abundances are invited to perform their own fit to η by following the simple prescription given here.

Before performing the χ^2 fit, it is useful to get an idea of what one should expect by comparing the data with the theoretical predictions at various values of η . Fig. 5 shows the theoretical predictions for the abundances Y_2 , Y_4 , and Y_7 in the three possible planes (Y_i, Y_j) , for representative values of $x \equiv \log_{10}(\eta/10^{-10})$. The corresponding 1σ error ellipses show clearly the size and the correlation of the “theoretical” errors. Fig. 6 shows, in the same planes as in Fig. 5, the 1σ error ellipses associated with the data sets “A” and “B”. Clearly the former prefers $\eta \sim 2 \times 10^{-10}$ while the latter favours $\eta \sim (4\text{--}5) \times 10^{-10}$.

A more precise estimate of the likely range of η is obtained, as anticipated, through a χ^2 fit. The results are shown in Fig. 7. The value of χ^2_{\min} is almost zero for the fit to data set “A”, indicating very good agreement between theory and observations, while it is somewhat larger for data set “B”. Note that the characteristic minimum in the ^7Li curve at $\eta \approx 2.6 \times 10^{-10}$ (see bottom panel of Fig. 1) allows its measured abundance to be compatible with both high D/low ^4He (data set “A”) or low D/high ^4He (data set “B”). The 95% C.L. ranges allowed by each of the two data sets, as obtained by cutting the curves at $\Delta\chi^2 = \chi^2 - \chi^2_{\min} = 3.84$, are:

$$\text{Data set A : } \eta = 1.78_{-0.34}^{+0.54} \times 10^{-10}, \quad (16)$$

$$\text{Data set B : } \eta = 5.13_{-0.66}^{+0.72} \times 10^{-10}. \quad (17)$$

The range for case “A” agrees very well with the 95% C.L. range estimated in Ref. [26] with the same inputs but with a different method (Monte Carlo + maximum likelihood). Of course, the incompatibility between the above two ranges of η reflects the incompatibility between the input abundance data within their stated errors.

IV. ROLE OF DIFFERENT REACTIONS IN LIGHT ELEMENT NUCLEOSYNTHESIS

The role of the different nuclear reactions rates listed in Table II in the synthesis of the light elements can be studied by “perturbing” the values of the input reaction rates and observing their effect on the predicted abundances. More precisely, one can study the contribution to the total uncertainty σ_i of Y_i induced by a $+1\sigma$ shift of R_k :

$$R_k \rightarrow R_k + \Delta R_k \implies Y_i \rightarrow Y_i + \delta Y_i. \quad (18)$$

Within our approach, this can be done very easily using Eq. (3), with the ΔR_k ’s from Table II. Of course, the results depend on the value chosen for η . To illustrate various trends, we choose the best-fit values $\eta = 1.78 \times 10^{-10}$ and $\eta = 5.13 \times 10^{-10}$, corresponding to data sets “A” and “B” respectively.

Figs. 8 and 9 show the deviations δY_i (normalized to the total error σ_i) induced by $+1\sigma$ shifts in the R_k ’s, plotted in the same set of planes as used for Figs. 5 and 6. The stochastic combination of the deviation vectors (i.e., a “random walk” of steps $\delta Y_i/\sigma_i$) leads to the 1σ error ellipses shown in these figures. Several interesting conclusions can be drawn from this exercise. As expected, the uncertainty in the weak interaction rate R_1 has the greatest

impact on Y_4 , since essentially all neutrons end up being bound in ^4He . However at the lower value of η (Fig. 8), the uncertainty in R_2 — the “deuterium bottleneck” — plays an equally important role as R_1 in determining Y_4 because nuclear burning is less complete here than at high η (Fig. 9). Similarly with reference to the reaction rates R_7 , $R_{10} - R_{12}$ which synthesize ^7Li , at low η it is the competition between R_7 and R_{11} which largely determines Y_7 , while at high η it is the competition between R_{10} and R_{12} . The anticorrelation between Y_4 and Y_2 is driven mainly by R_2 at low η and, to a lesser extent, by R_4 and R_5 , while the reverse is the case at high η . The anticorrelation between Y_4 and Y_7 at low η is also basically driven by R_2 , while the correlation at high η is due to both R_2 and R_4 . Thus we have a direct visual basis for assessing in what direction the output abundances Y_i are pulled by possible changes in the input cross sections R_k .

V. CONCLUSIONS

We have shown that a simple method based on linear error propagation allows us to quantify the uncertainties associated with the elemental abundances expected from big bang nucleosynthesis, in excellent agreement with the results obtained from Monte Carlo simulations. This method makes transparent which nuclear reaction rate is mainly responsible for the uncertainty in the abundance of a given element. If determinations of the primordial abundances improve to the point where the observational errors become smaller than the theoretical uncertainties (say for ^7Li), this will enable attention to be focussed on the particular reaction rate whose value needs to be experimentally better known.

We have also demonstrated that for standard BBN, our method enables the use of simple χ^2 statistics to obtain the best-fit value of η from the comparison of theory and observations. At present there are conflicting claims regarding the primordial abundances of, particularly, D and ^4He , and different choices of input data sets imply values of η differing by a factor of ~ 3 . However this quantity can also be determined through measurements of the angular anisotropy of the cosmic microwave background (CMB) on small angular scales. Within a decade the forthcoming all-sky surveyors MAP and PLANCK are expected to pinpoint the nucleon density to within $\sim 5\%$ [35]. Such measurements probe the acoustic oscillations of the coupled photon-matter plasma at the (re)combination epoch and will thus provide an independent check of BBN, assuming η did not change significantly between the two epochs.⁷ Nevertheless precise measurements of light element abundances, particularly ^4He , are still crucial because they provide a unique probe of physical conditions, in particular the expansion rate at the BBN epoch. To illustrate, if η was determined by the CMB measurements to be $\approx 2 \times 10^{-10}$ as indicated by the comparison of data set “A” with BBN theory, but the abundance of ^4He was established to be actually closer to its higher

⁷New physics beyond the Standard Model can change η , e.g. by increasing the photon number through massive particle decay [36] or, more exotically, by *decreasing* the photon number through photon mixing with a shadow sector [37]. However such possibilities are strongly constrained by the absence of distortions in the Planck spectrum of the CMB [38] and also, in the latter case, by the absence of Sakharov oscillations in the power spectrum of large-scale structure [39].

value of $\approx 24\%$ in data set “B”, *this would be a strong indication that the expansion rate during BBN was higher than in the standard case with $N_\nu = 3$ neutrinos*. Although the number of $SU(2)$ doublet neutrinos is indeed 3, there are many light particles expected in extensions of the Standard Model, e.g. singlet neutrinos, which can speed up the expansion rate during nucleosynthesis [19]. The generalization of our method to such non-standard cases is straightforward and it is clear that BBN analyses will continue to be important in this regard for both particle physics and cosmology.

ACKNOWLEDGMENTS

E.L. thanks the Department of Physics at Oxford University for hospitality during the early stages of this work. S.S. and F.V. thank the organizers and participants in the International Workshop on *Synthesis of Light Nuclei in the Early Universe* held at ECT, Trento in June 1997 for useful discussions. We thank Rob Lopez for helpful feedback. This work was supported by the EC Theoretical Astroparticle Network CHRX-CT93-0120 (DG12 COMA).

TABLES

TABLE I. The four light elemental abundances Y_i considered in this work. Alternative symbols used in the literature are indicated in parentheses.

Symbol	... or	Definition
Y_4	(Y_p)	${}^4\text{He}$ mass fraction
Y_2	(y_{2p})	D/H (by number)
Y_3	(y_{3p})	${}^3\text{He}/\text{H}$ (by number)
Y_7	(y_{7p})	${}^7\text{Li}/\text{H}$ (by number)

TABLE II. The BBN reaction rates R_k and their 1σ uncertainties $\pm\Delta R_k$ adopted in this work. The numbering follows Ref. [16] while the reference “unit” values ($R_k \equiv 1$) correspond to the rates in Ref. [17].

k	Reaction	R_k	$\pm\Delta R_k$
1	$\text{n} \rightarrow \text{p} \text{ e} \bar{\nu}_e$	0.9979	± 0.0021
2	$\text{p}(\text{n},\gamma)\text{d}$	1	± 0.07
3	$\text{d}(\text{p},\gamma){}^3\text{He}$	1	± 0.10
4	$\text{d}(\text{d},\text{n}){}^3\text{He}$	1	± 0.10
5	$\text{d}(\text{d},\text{p})\text{t}$	1	± 0.10
6	$\text{t}(\text{d},\text{n}){}^4\text{He}$	1	± 0.08
7	$\text{t}(\alpha,\gamma){}^7\text{Li}$	1	± 0.26
8	${}^3\text{He}(\text{n},\text{p})\text{t}$	1	± 0.10
9	${}^3\text{He}(\text{d},\text{p}){}^4\text{He}$	1	± 0.08
10	${}^3\text{He}(\alpha,\gamma){}^7\text{Be}$	1	± 0.16
11	${}^7\text{Li}(\text{p},\alpha){}^4\text{He}$	1	± 0.08
12	${}^7\text{Be}(\text{n},\text{p}){}^7\text{Li}$	1	± 0.09

TABLE III. Polynomial fit to the central value of the elemental abundances, $Y_i = a_0 + a_1x + a_2x^2 + a_3x^3 + a_4x^4 + a_5x^5$, with $x \equiv \log_{10}(\eta/10^{-10})$ in the range 0–1. The abundances were obtained using the BBN computer code [16] with the input R_k ’s as in Table II. The value of Y_4 has been corrected using the prescription of Ref. [19]. The accuracy of the fit is better than 1/25 of the total theoretical uncertainty for each Y_i .

	a_0	a_1	a_2	a_3	a_4	a_5
$Y_2 \times 10^3$	+0.4808	-1.8112	+3.2564	-3.3525	+1.8834	-0.4458
$Y_3 \times 10^5$	+3.4308	-6.1701	+8.1311	-9.7612	+7.7018	-2.5244
$Y_4 \times 10^1$	+2.2305	+0.5479	-0.6050	+0.6261	-0.3713	+0.0949
$Y_7 \times 10^9$	+0.5369	-2.8036	+7.6983	-12.571	+12.085	-3.8632

TABLE IV. Polynomial fits to the logarithmic derivatives, $\lambda_{ik}(x) = a_0 + a_1x + a_2x^2 + a_3x^3 + a_4x^4 + a_5x^5$, as functions of $x \equiv \log_{10}(\eta/10^{-10}) \in [0, 1]$ (see Fig. 2). In most cases, polynomials of degree < 5 provide sufficiently accurate fits. Only non-negligible logarithmic derivatives are tabulated.

	k	a_0	a_1	a_2	a_3	a_4	a_5
λ_{2k}	1	+0.7130	-0.7964	+0.4577	+0.0914	0	0
	2	-0.7025	+0.2611	+1.2008	-0.8934	0	0
	3	-0.0189	-0.1879	+0.2502	-0.6806	0	0
	4	-0.4228	-0.1698	+0.0207	+0.0247	0	0
	5	-0.4138	-0.1477	+0.1103	+0.0010	0	0
	8	-0.0073	-0.0003	+0.0801	-0.0416	0	0
	9	-0.0011	-0.0348	+0.0592	-0.0511	0	0
λ_{3k}	1	+0.0940	+0.1892	-0.1484	-0.0199	0	0
	2	+0.0981	+0.9948	-3.1667	+3.4108	-1.2845	0
	3	+0.0610	+0.1640	+0.5368	-0.2605	0	0
	4	+0.3050	+0.0805	-0.4208	+0.1555	0	0
	5	-0.5118	+0.1274	+0.4081	-0.2106	0	0
	6	-0.0327	+0.0829	-0.0939	+0.0362	0	0
	8	-0.5580	-0.0287	+1.3574	-0.8735	0	0
	9	-0.1080	-0.5089	-1.0157	+0.8163	0	0
	12						
λ_{4k}	1	+0.8138	-0.1465	+0.0408	0	0	0
	2	+0.0610	-0.1962	+0.2416	-0.1049	0	0
	4	+0.0082	-0.0058	+0.0034	0	0	0
	5	+0.0075	-0.0058	+0.0034	0	0	0
λ_{7k}	1	+1.9638	+1.8520	-19.721	+27.542	-11.041	0
	2	-0.9214	-1.6472	+5.6187	+54.059	-112.80	+56.426
	3	+0.0500	-1.0433	+4.1384	-2.4441	0	0
	4	+0.1734	-2.7428	+11.209	-10.736	+2.5263	0
	5	+0.1837	-0.0875	+0.0158	-0.1350	0	0
	6	-0.9877	-0.8168	+6.1555	-4.4380	0	0
	7	+0.9644	+0.6888	-5.6151	+4.0284	0	0
	8	+0.0529	+0.6318	-3.3995	+2.5754	0	0
	9	-0.0764	+0.3017	-2.9632	+1.9311	0	0
	10	+0.0690	-1.5360	+9.5808	-10.168	+2.9807	0
	11	-1.4095	-0.3543	+6.4780	-4.7956	0	0
	12	-0.0043	-0.3779	+7.7358	-42.390	+61.401	-26.778

REFERENCES

- [1] D. N. Schramm and M. S. Turner, Rev. Mod. Phys. (Colloquia) **70**, 303 (1998).
- [2] S. Burles and D. Tytler, astro-ph/9712265, in *Primordial Nuclei and their Galactic Evolution*, Proc. ISSI Workshop (Bern, 1997) edited by N. Prantzos, M. Tosi, and R. von Steiger (Kluwer, Dordrecht), to appear.
- [3] J. K. Webb, R. F. Carswell, K. M. Lanzetta, R. Ferlet, M. Lemoine, and A. Vidal-Madjar, astro-ph/9710089, in *Structure and Evolution of the Intergalactic Medium from QSO Absorption Line Systems*, Proceedings of the 13th IAP Workshop (Paris, 1997), edited by P. Petitjean and S. Charlot (Nouvelles Frontières, Paris), to appear.
- [4] D. S. Balser, T. M. Bania, R. T. Rood and T. M. Wilson, *Astrophys. J.* **430**, 667 (1994).
- [5] G. Gloeckler and J. Geiss, *Nature (London)* **381**, 210 (1996).
- [6] K. A. Olive, G. Steigman and E. D. Skillman, *Astrophys. J.* **483**, 788 (1997).
- [7] Y. I. Izotov, T. X. Thuan, and V. A. Lipovetsky, *Astrophys. J. Suppl.* **108**, 1 (1997).
- [8] S. G. Ryan, T. C. Beers, C. P. Deliyannis and J. A. Thorburn, *Astrophys. J.* **458**, 543 (1996).
- [9] P. Bonifacio and P. Molaro, *Mon. Not. Roy. Astron. Soc.* **285**, 847 (1997).
- [10] P. Molaro, astro-ph/9709245, in *From Quantum Fluctuations to Cosmological Structures*, Proc. 1st Moroccan International Astronomy School (Casablanca, 1996), edited by D. Valls-Gabaud *et al.*, ASP Conf. Ser. **126**, p. 103.
- [11] C. Hogan, astro-ph/9712031, in *Primordial Nuclei and their Galactic Evolution*, Proc. ISSI Workshop (Bern, 1997) edited by N. Prantzos, M. Tosi, and R. von Steiger (Kluwer, Dordrecht), to appear.
- [12] S. A. Levshakov, W. H. Kegel, and F. Takahara, astro-ph/9712136, in *Toward the first light of HDS*, Proc. SUBARU HDS Workshop (Tokyo, 1997), to appear.
- [13] J. A. Bernstein, L. S. Brown, and G. Feinberg, *Rev. Mod. Phys.* **61**, 25 (1989).
- [14] R. Esmailzadeh, G. D. Starkman, and S. Dimopoulos, *Astrophys. J.* **378**, 504 (1991).
- [15] R. V. Wagoner, *Astrophys. J.* **179**, 343 (1973).
- [16] L. Kawano, Report No. Fermilab-Pub-88/34-A, 1988 (unpublished); Report No. Fermilab-Pub-92/04-A, 1992 (unpublished).
- [17] M. S. Smith, L. H. Kawano, and R. A. Malaney, *Astrophys. J. Suppl.* **85**, 219 (1993).
- [18] K. A. Olive, astro-ph/9712160, in Proc. *TAUP'97*, 5th International Workshop on Topics in Astroparticle and Underground Physics (Laboratori Nazionali del Gran Sasso, Assergi, 1997) to appear.
- [19] S. Sarkar, *Rep. Prog. Phys.* **59** (1996), 1493.
- [20] L. M. Krauss and P. Romanelli, *Astrophys. J.* **358**, 47 (1990).
- [21] P. J. Kernan and L. M. Krauss, *Phys. Rev. Lett.* **72**, 3309 (1994).
- [22] P. J. Kernan and L. M. Krauss, Case Western Reserve University report No. CWRU-P2-94, astro-ph/9402010. This report, published in an abridged version as Ref. [21], contains additional numerical results relevant for comparison with our work.
- [23] L. M. Krauss and P. J. Kernan, *Astrophys. J. Lett.* **432**, 79 (1994); *Phys. Lett. B* **347**, 347 (1995).
- [24] C. J. Copi, D. N. Schramm, and M. S. Turner, *Science* **267**, 192 (1995); *Phys. Rev. Lett.* **75**, 3981 (1995).
- [25] N. Hata, R. J. Scherrer, G. Steigman, D. Thomas, T. P. Walker, S. Bludman, and P.

- Langacker, Phys. Rev. Lett. **75**, 3977 (1995); N. Hata, R. J. Scherrer, G. Steigman, D. Thomas, and T. P. Walker, Astrophys. J. **458**, 637 (1996); N. Hata, G. Steigman, S. Bludman, and P. Langacker, Phys. Rev. D **55**, 540 (1997).
- [26] K. A. Olive and D. Thomas, Astropart. Phys. **7**, 27 (1997). See also B. D. Fields and K. A. Olive, Phys. Lett. B **368**, 103 (1996); B. D. Fields, K. Kainulainen, K. A. Olive, and D. Thomas, New Astron. **1**, 77 (1996).
- [27] R. M. Barnett *et al.*, Phys. Rev. D **54**, 1 (1996), and 1997 off-year partial update for the 1998 edition available on the Particle Data Group WWW pages (URL: <http://pdg.lbl.gov/>). This update includes the revised Penning-trap measurement of Ref. [28].
- [28] $\tau_n = 889.2 \pm 4.8$ s, J. Byrne, *et al.*, Europhys. Lett. **33**, 187 (1996). Here the authors revise and replace their previous estimate ($\tau_n = 893.5 \pm 5.3$ s) which appeared in J. Byrne *et al.*, Phys. Rev. Lett. **65**, 289 (1990).
- [29] W. T. Eadie, D. Drijard, F. E. James, M. Roos, and B. Sadoulet, *Statistical Methods in Experimental Physics* (North Holland, Amsterdam and London, 1971).
- [30] P. J. Kernan, *PhD thesis*, Ohio State University (1993).
- [31] R. Lopez, private communication.
- [32] J. N. Bahcall and R. N. Ulrich, Rev. Mod. Phys. **60**, 297 (1988); J. N. Bahcall and W. C. Haxton, Phys. Rev. D **40**, 931 (1989); X. Shi and D. N. Schramm, Phys. Lett. B **283**, 305 (1992); L. M. Krauss, E. Gates, and M. White, Phys. Lett. B **299**, 94 (1993).
- [33] G. L. Fogli and E. Lisi, Astropart. Phys. **3**, 185 (1995); N. Hata and P. Langacker, Phys. Rev. D **50**, 632 (1994); E. Gates, L. M. Krauss, and M. White, Phys. Rev. D **51**, 2631 (1995).
- [34] P. J. Kernan and S. Sarkar, Phys. Rev. D **54**, R3681 (1996); S. Sarkar, astro-ph/9611232, in *Aspects of Dark Matter in Astro- and Particle Physics*, edited by H. V. Klapdor-Kleingrothaus and Y. Ramachers (World Scientific, 1997) p. 235.
- [35] L. Knox, Phys. Rev. D **52** 4307 (1995); G. Jungman, M. Kamionkowski, A. Kosowsky, and D. N. Spergel, Phys. Rev. D **54** 1332 (1996); M. Zaldarriaga, D. N. Spergel and U. Seljak, Astrophys. J. **488** 1 (1997); J. R. Bond, G. Efstathiou and M. Tegmark, Mon. Not. R. Astron. Soc. **291**, L33 (1997).
- [36] K. Sato and M. Kobayashi, Prog. Theor. Phys. **58**, 1775 (1977); D. A. Dicus, E. W. Kolb, V. L. Teplitz and R. V. Wagoner, Phys. Rev. D **17**, 1529 (1978).
- [37] J. G. Bartlett and L. Hall, Phys. Rev. Lett. **66**, 541 (1991).
- [38] J. Ellis, G. B. Gelmini, D. V. Nanopoulos, J. Lopez and S. Sarkar, Nucl. Phys. B **373**, 399 (1992); W. Hu and J. Silk, Phys. Rev. Lett. **70**, 2661 (1993).
- [39] M. Birkel and S. Sarkar, Phys. Lett. B **408**, 59 (1997). See also D. J. Eisenstein, W. Hu, J. Silk and A. Szalay, Astrophys. J. Lett. **494**, L1 (1998).

FIGURES
Light element abundances $Y_i(\eta) \pm 2\sigma_i(\eta)$

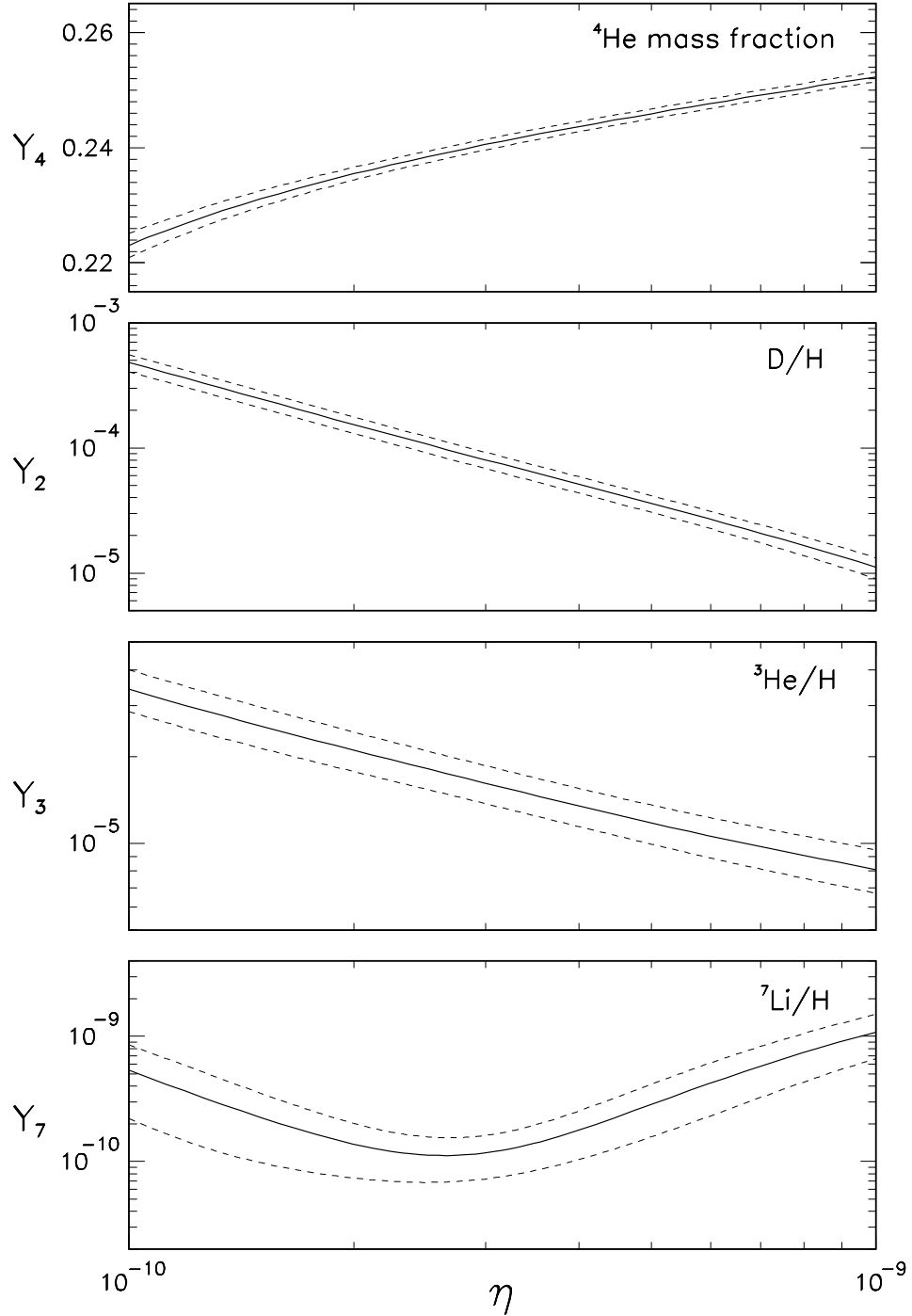


FIG. 1. Primordial abundances Y_i (solid lines) and their $\pm 2\sigma$ bands (dashed lines), as functions of the nucleon-to-photon ratio η .

$$\text{Logarithmic derivatives } \lambda_{ik}(\eta) = \frac{\partial \ln Y_i(\eta)}{\partial \ln R_k}$$

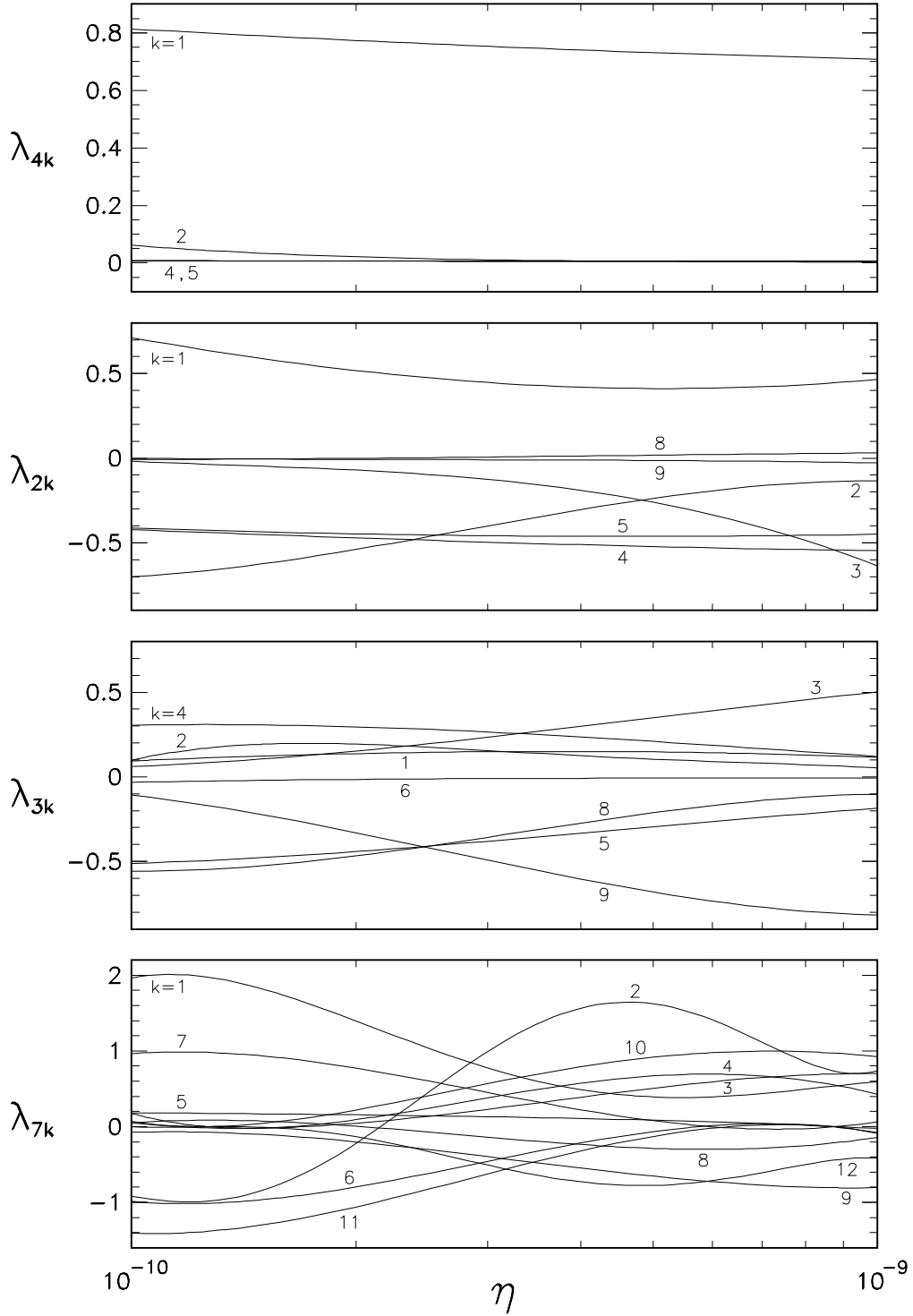


FIG. 2. Logarithmic derivatives λ_{ik} of the abundances Y_i with respect to the reaction rates R_k , as functions of η .

Abundance uncertainties and correlations
 $(2, 3, 4, 7 = D, {}^3\text{He}, {}^4\text{He}, {}^7\text{Li})$

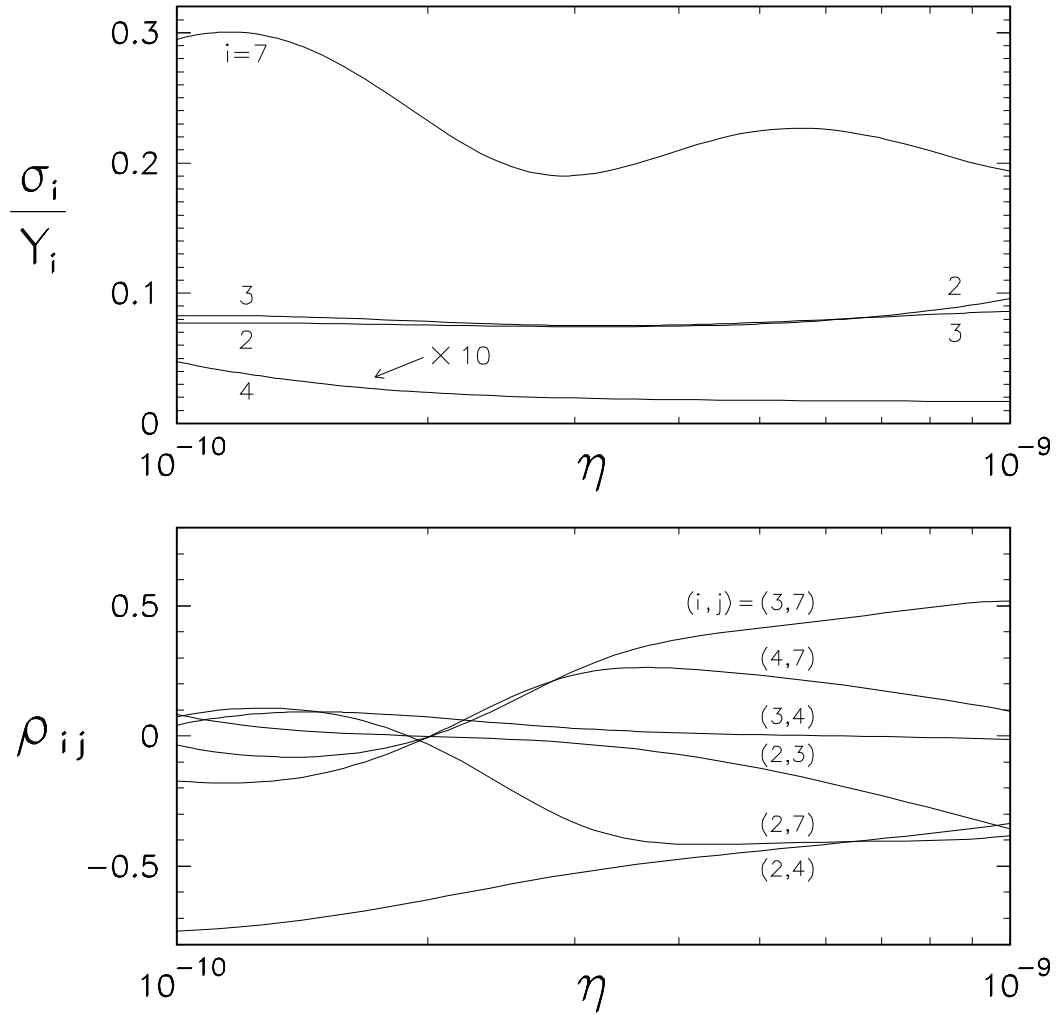


FIG. 3. Fractional abundance uncertainties σ_i/Y_i (upper panel) and their correlations ρ_{ij} (lower panel), as functions of η .

MonteCarlo vs Analytic estimate

(2, 3, 2+3, 4, 7 = D, ${}^3\text{He}$, D+ ${}^3\text{He}$, ${}^4\text{He}$, ${}^7\text{Li}$)

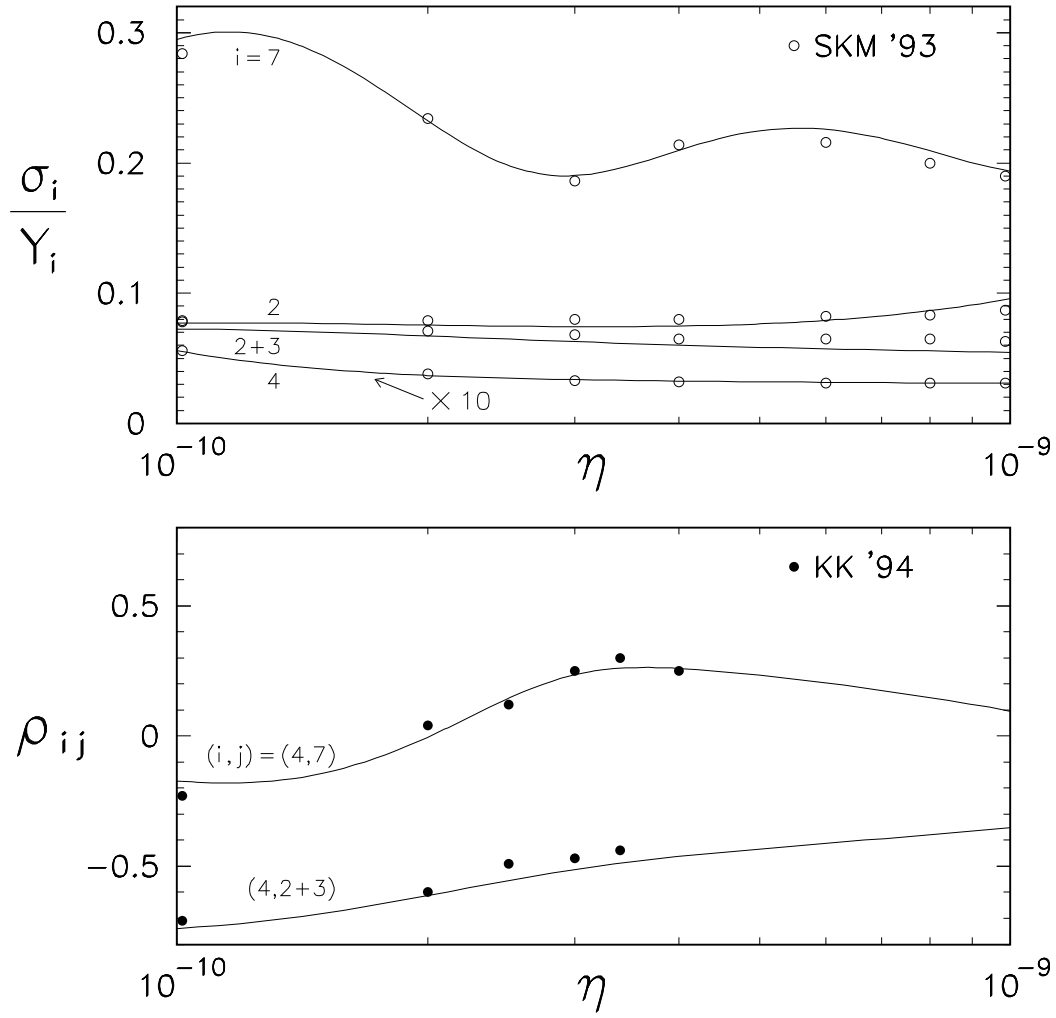


FIG. 4. Monte Carlo estimates of σ_i/Y_i (SKM '93 [17], dots) and ρ_{ij} (KK '94 [22], dots), compared with our analytic evaluation (solid lines), using the same inputs.

Standard BBN predictions and 1σ uncertainties

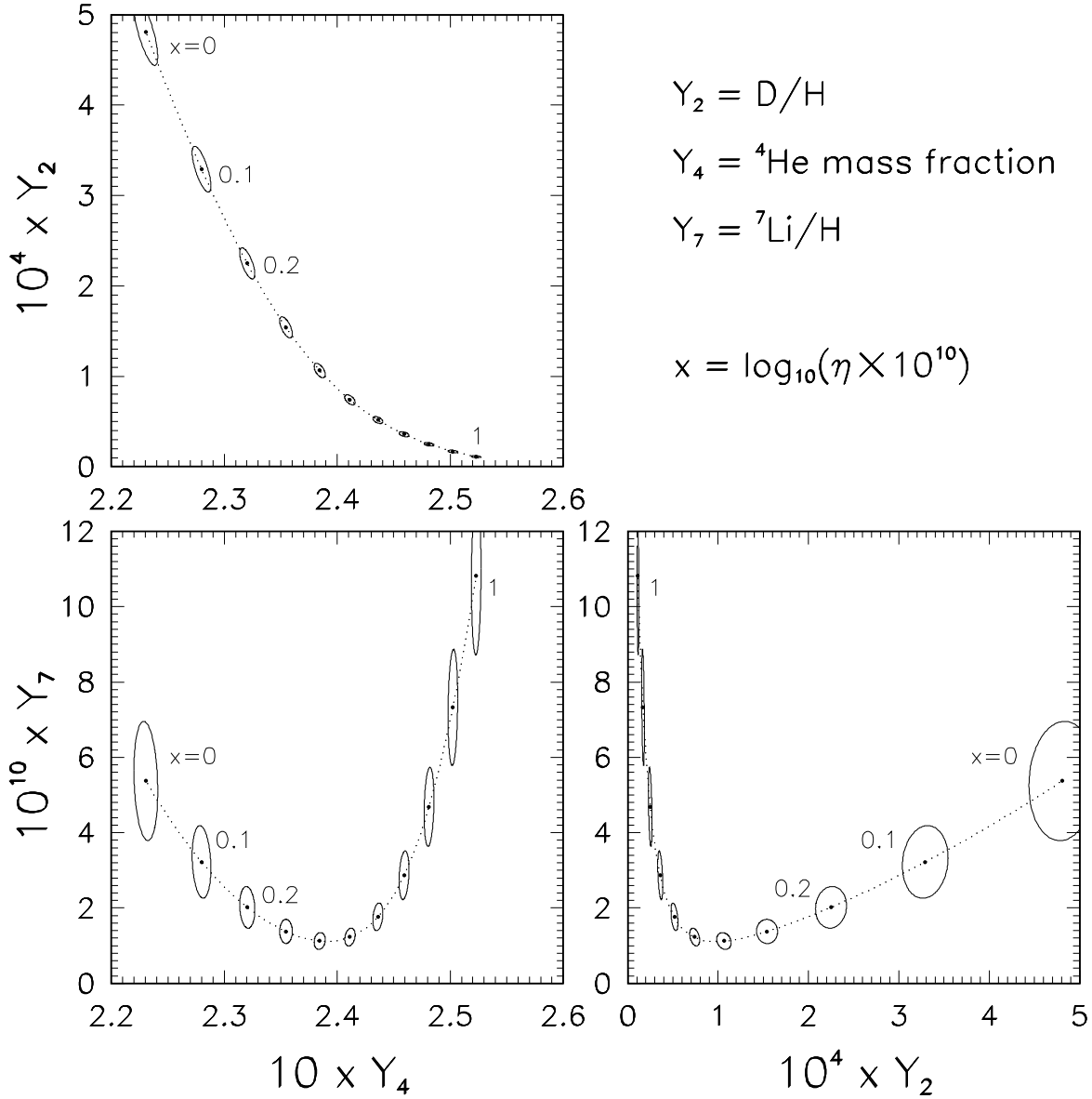


FIG. 5. Standard BBN predictions in the 2-dimensional planes defined by the abundances Y_2 , Y_4 , and Y_7 , as functions of $x \equiv \log_{10}(\eta/10^{-10})$ (dotted lines). The solid lines represent our estimate of the 1σ error ellipses at $x = 0, 0.1, 0.2, \dots, 1$.

Big Bang Nucleosynthesis – Theory vs Data

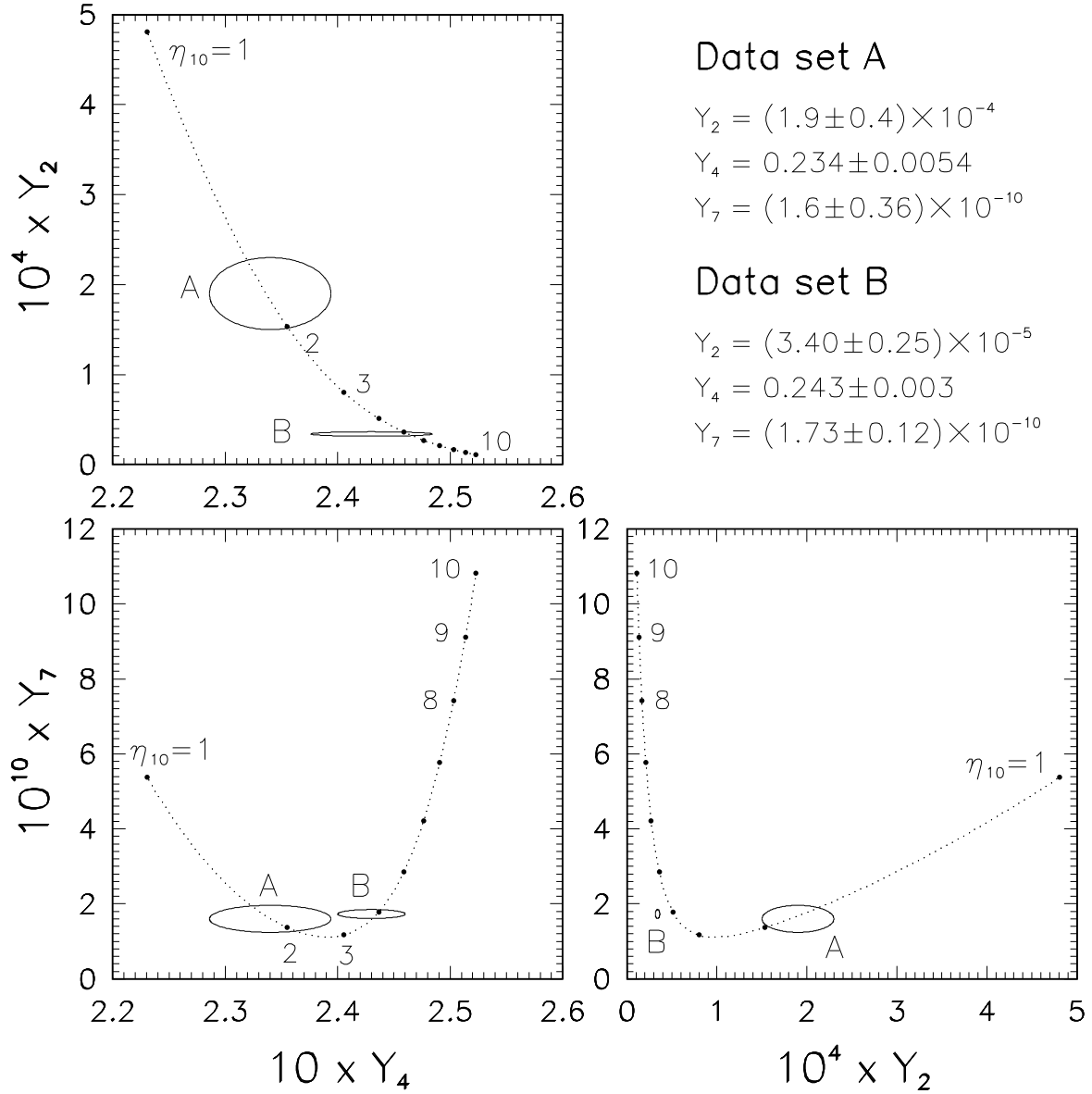


FIG. 6. Standard BBN predictions (dotted lines) compared to two observational data sets (1σ ellipses A and B), in the same planes as in Fig. 5. The values $\eta_{10} = \eta/10^{-10} = 1, 2, 3, \dots, 10$ are marked by thick dots.

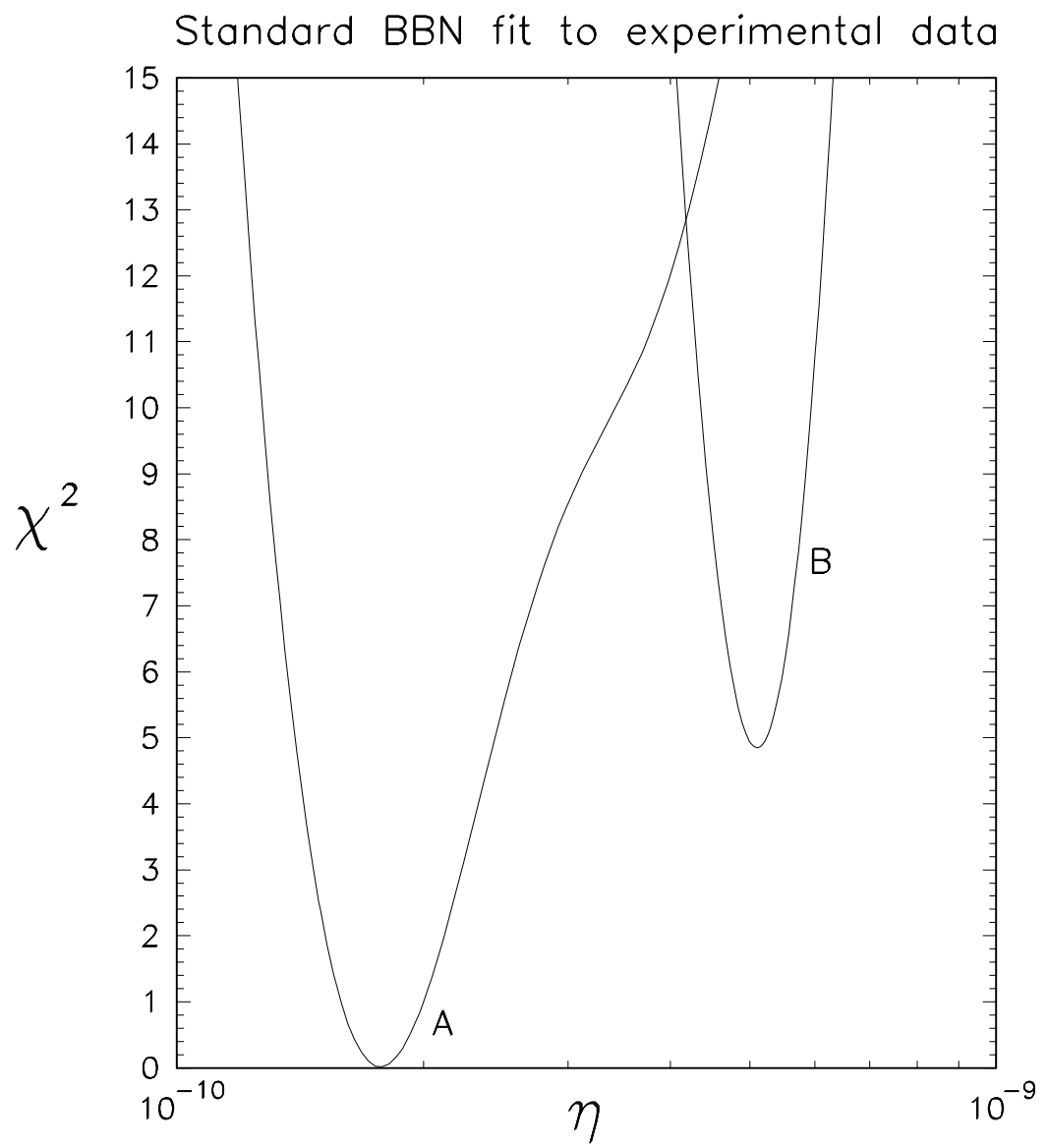


FIG. 7. Our χ^2 fit to the data sets A and B, including observational and (correlated) theoretical errors.

Big Bang Nucleosynthesis – Error Components at $\eta = 1.78 \times 10^{-10}$

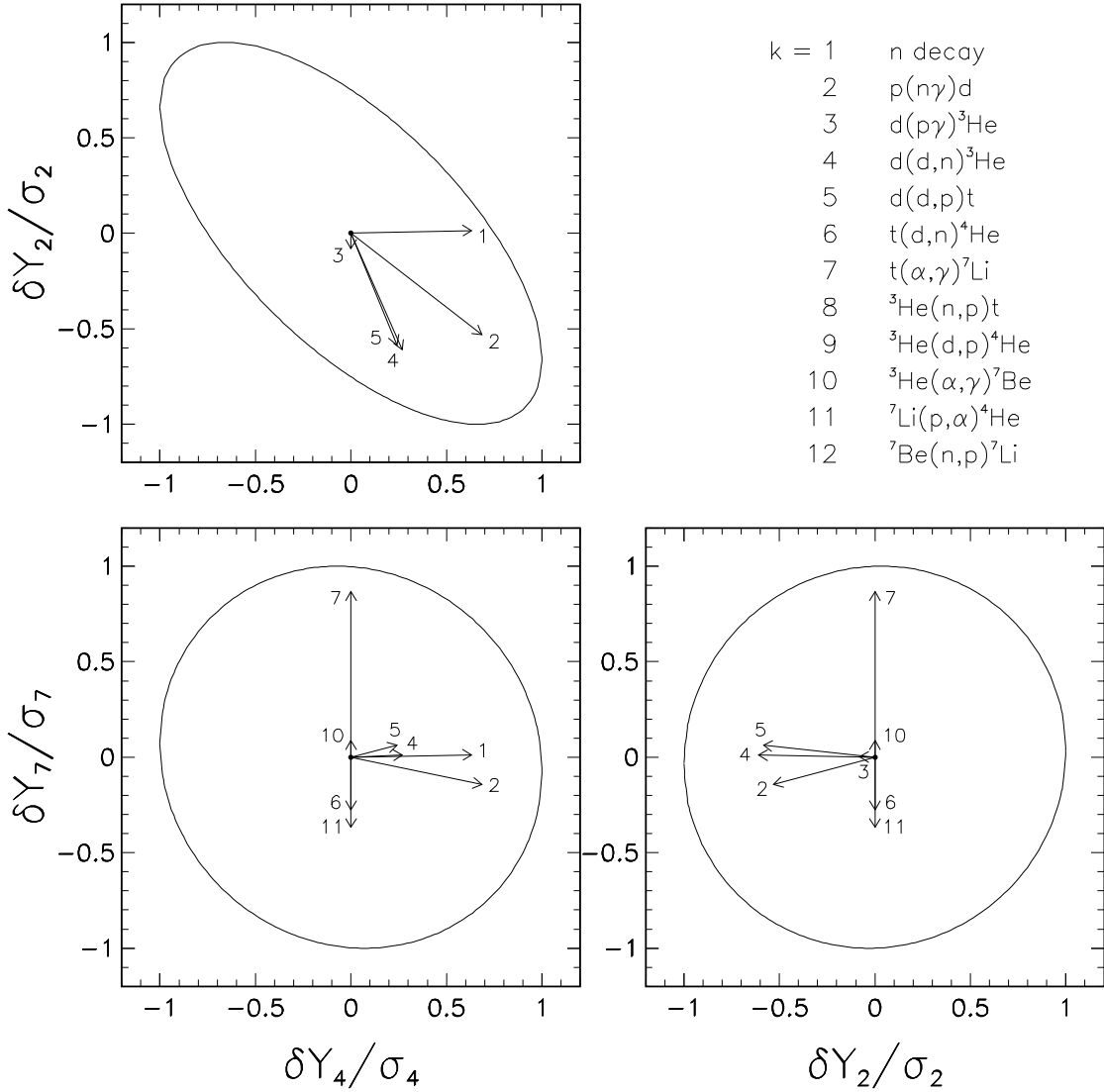


FIG. 8. Individual contributions of different reaction rates R_k to the uncertainties in Y_2 , Y_4 , and Y_7 , normalized to the corresponding total errors σ_2 , σ_4 , and σ_7 , for $\eta = 1.78 \times 10^{-10}$. Each arrow corresponds to the shift δY_i induced by a $+1\sigma$ shift of R_k . Some small error components have not been plotted.

Big Bang Nucleosynthesis – Error Components at $\eta = 5.13 \times 10^{-10}$

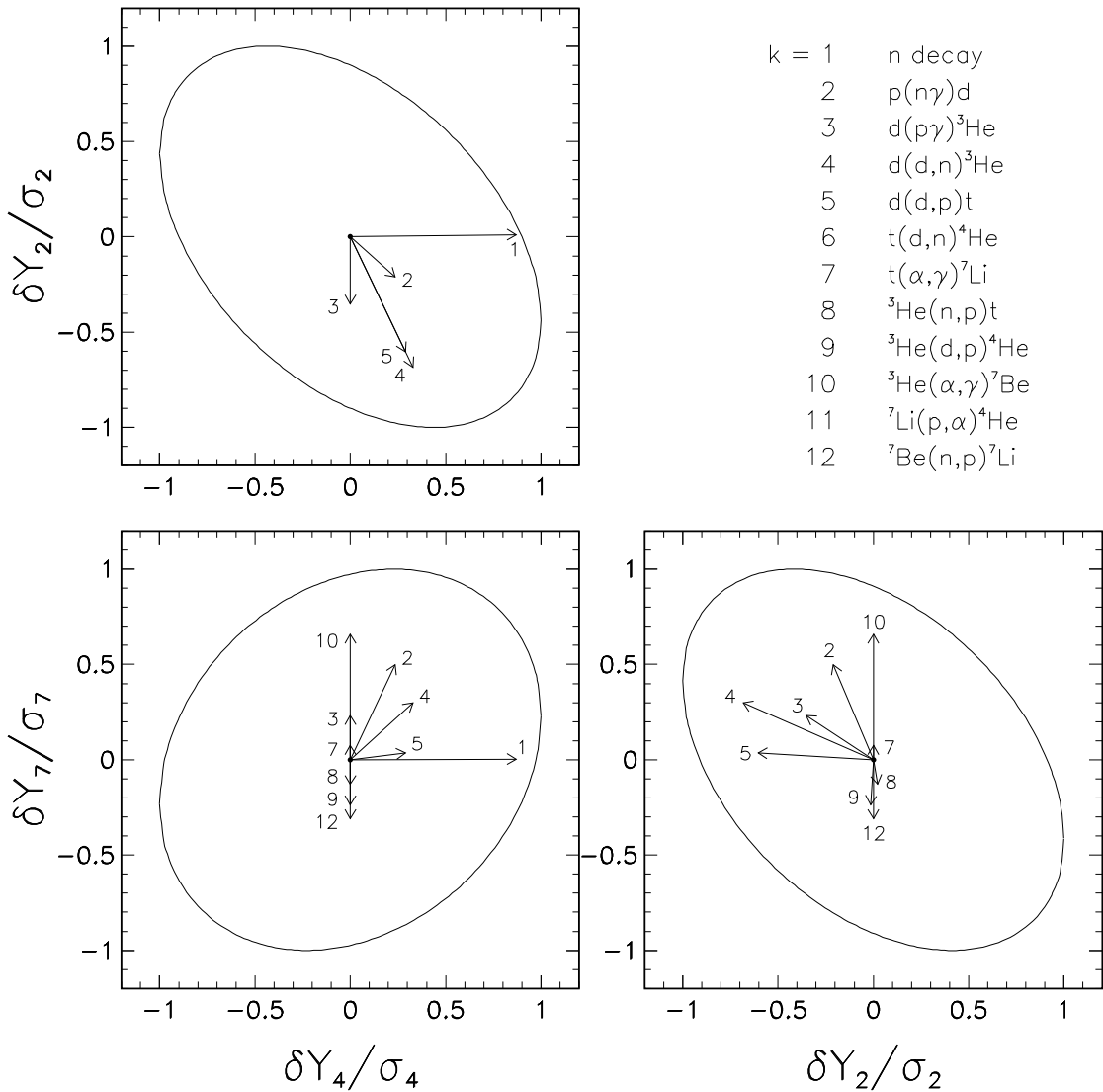


FIG. 9. Same as Fig. 8, but for $\eta = 5.13 \times 10^{-10}$.